Wiley Online Library
Early View publication on www.wileyonlinelibrary.com
(issue and page numbers not yet assigned;
citable using Digital Object Identifier – DOI)

Phys. Status Solidi C, 1–4 (2015) / DOI 10.1002/pssc.201400271

physica status solidi c
www.pss-c.com
current topics in solid state physics

Study of the synthesis of self-assembled tin disulfide nanoparticles prepared by a low-cost process

Arturo Méndez-López[*, 1], Arturo Morales-Acevedo[1], Yuliana de Jesús Acosta-Silva[2], Hironori Katagiri[3], Yasuhiro Matsumoto[1], Orlando Zelaya-Angel[2], and Mauricio Ortega-López[1]

[1] Sección de Electrónica del Estado Solido (SEES), Depto. de Ingeniería Eléctrica, Centro de Investigación y de Estudios Avanzados del Instituto Politécnico Nacional, Avenue IPN No. 2508, 07360 Mexico City, DF, Mexico
[2] Depto. de Física, Centro de Investigación y de Estudios Avanzados del Instituto Politécnico Nacional, Avenue IPN No. 2508, 07360 Mexico City, DF, Mexico
[3] Nagaoka National College of Technology, 888 Nishikatakai, Nagaoka, Niigata 940-8532, Japan

Received 29 September 2014, revised 6 February 2015, accepted 11 March 2015
Published online 20 April 2015

Keywords SnS_2, colloidal synthesis, hot-injection technique, semiconductors, nanostructures

* Corresponding author: e-mail amendez@cinvestav.mx, Phone: + 52 55 57 47 37 75, Fax: +52 55 57 47 38 00

Oleylamine-capped tin disulfide nanoparticles were prepared by the hot-injection method using tin (II) chloride ($SnCl_2.5H_2O$) and thioacetamide as tin (II) and sulfur precursors, respectively. The as-prepared nanoparticles were rinsed with ethanol or toluene, and their structural and morphological were assessed by X-ray diffraction, Raman spectroscopy, scanning electron microscopy and transmission electron microscopy. The obtained nanoparticles were single-phase SnS_2 with hexagonal structure. These nanoparticles self-assembled to produce spherical 40-50 nm nanostructures after ethanol evaporation, whilst rhombohedral-shaped nanostructures or round-edge nanoribbons were produced after the toluene evaporation.

1 Introduction The best solar cell adopting inorganic nanophase as the electron acceptor demonstrated a power conversion efficiency exceeding 3% using CdSe tetrapods [1]. However, compared with this toxic material, a non-toxic, environment-friendly alternative may be more attractive for future application in this kind of cells.

SnS_2 is a layered semiconductor which belongs to the CdI_2-type structure with a band-gap of 2-3 eV [2]. A broad band-gap material leads to high photo-conductance [3] and makes it a candidate for solar cells and opto-electronic devices [4]. Compared with other inorganic nanoparticles containing Cd, SnS_2 is easy to prepare, nontoxic, environment-friendly, and raw materials are abundant on earth. SnS_2 nanomaterials have been widely used for a variety of industrial and technical applications, for example, semiconductor [5], Li-ion battery anode material [6], solar cells [7], etc. Various morphologies of SnS_2 materials including nanoplates, nanorods, nanobelts, nanoflowers and nanotubes have been fabricated using different synthesis methods [8, 9].

A variety of methods have been developed for the syntheses of SnS_2, such as direct combination of the constituent elements [10], solid-state metathesis [5], vapor transport [11], these synthetic processes require high temperature or expensive instruments. Mild syntheses approaches, hydrothermal and solvothermal methods [12, 13], successive ionic layer adsorption and reaction (SILAR) [14], can produce relative big SnS_2 crystals with several hundred nanometers long and wide, even to micrometers, and so it is difficult to obtain pure nanocrystals (NCs) of this material.

The Hot-injection method [15] has been widely used to synthesize semiconductor nanomaterials because of its versatility to control high crystalline and monodisperse nanoparticle production [16].

In this work, we report hot-injection method for the preparation of monodisperse SnS_2 nanoparticles, simply by mixing $SnCl_2$ and thioacetamide with oleylamine at 230 °C. In the present work, oleylamine passivates the surface of grown nanoparticles and prevent agglomeration. Our method can be used to prepare large scale highly poly-

disperse SnS_2 nanoparticles at high temperature. The prepared nanoparticles were dispersed in ethanol or toluene after the nanoparticles settle down themselves at the bottom of the container, so it is simple to purify them. Also, the structure and morphology of the products have been characterized by X-ray diffraction (XRD), micro-Raman spectroscopy, scanning electron microscopy (SEM) and transmission electron microscopy (TEM).

2 Experimental

2.1 Synthesis of SnS_2 nanoparticles via hot-injection method SnS_2 nanoparticles were synthesized by the hot-injection method. In a typical synthesis, 0.26 g Tin (II) chloride dihydrate ($SnCl_2{\cdot}2H_2O$, 98.6%, Analyzer) was dissolved in 20 ml of oleylamine (OLA, $C_{18}H_{37}N$, 70%, Fluka) at room temperature. Then, the temperature of this mixture was raised to 170 °C under an inert nitrogen atmosphere for 60 min. Finally, the temperature of the mixture was raised to 230 °C. Then, 3 ml of OLA containing 0.15 g of thioacetamide (C_2H_5NS, TAA, 99.0%, Analytica) was dissolved at 40 °C until a transparent yellow solution was obtained. This solution was cooled back to room temperature and injected into the mixture quickly. The reaction was maintained at 230°C with an inert N_2 atmosphere and under continuous stirring for 24 h, and then cooled down to room temperature. The as-formed nanoparticles are isolated by precipitation with 20 ml ethanol or toluene followed by centrifugation at 4500 rpm for 30 min. The final product, SnS_2 nanoparticles are washed twice by means of solvent/antisolvent procedure using toluene/ethanol. We have observed that during the dispersion and purification of the oleylamine capped SnS_2 nanoparticles, it were precipitates more easily in ethanol than that in toluene due to the high thermal conductivity of ethanol At the end, the SnS_2 nanoparticles were suspended in 10 ml of ethanol or toluene used as solvent. The inkjet was deposited on the substrate by the drop coating technique. This post synthesis processes were conducted at room temperature. In our synthesis, oleylamine plays the dual role as reducing and stabilizing agent.

2.2 Characterization methods

2.2.1 X-ray diffraction (XRD) characterization methods The crystal structure of SnS_2 nanoparticles was investigated by X-ray diffraction (XRD) analysis, using the CuKα radiation with a wavelength of 1.5405 Å in the range: 20-70° on a PANalytical's X'pert PRO X-ray diffractometer.

2.2.2 Micro-Raman spectroscopy Raman spectroscopy (RS) of SnS_2 samples was carried out using a Jobin Horiba micro-spectrometer with a He-Ne laser that emitted at a wavelength of 632.8 nm and a power of 20 mW. The Raman spectra samples were measured at room temperature in a wavelength range between 200 and 600 nm, using a 50x objective to focalize the laser spot.

2.2.3 Scanning electron microscopy (SEM) The morphology of the SnS_2 samples were determined using an Auriga Zeiss 90-36 Scanning Electron Microscope.

2.2.4 Transmission electron microscopy (TEM) The micro-structures of SnS_2 were determined using a JEOL (model 2010) transmission electron microscope, operating with at 200 kV, with a point to point resolution of 0.18 nm.

3 Results and discussion

3.1 Scanning electron microscopy (SEM) The morphologies of SnS_2 nanoparticles washed in ethanol or toluene as solvent were investigated by SEM. SEM images revealed that the SnS_2 nanostructures washed with ethanol were spherical in shape (Fig. 1a). It is known that ethanol effectively removes the free oleylamine in the washing bath, while capping the SnS_2 nanoparticles and producing the nanoparticles flocculation. The obtained spherical clusters were 40-50 nm in size. In all cases, a polydisperse product was obtained, but the average cluster size could be controlled by modifying the reaction time. When toluene was used in the product rinsing, small oleylamine-capped SnS_2 nanoparticles were also obtained. These nanoparticles self-assembled to produce larger faceted nanostructures, about 350 nm in size, as indicated in Fig. 1b. A similar effect was observed in oleylamine capped YAG nanoparticles [17].

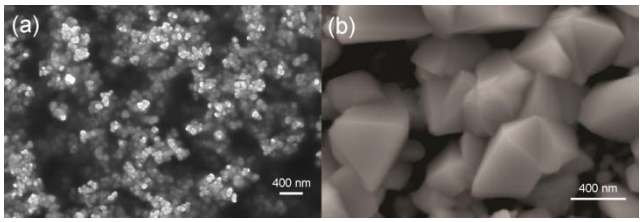

Figure 1 SEM images of the SnS_2 nanoparticles dispersed in (a) ethanol and (b) toluene.

3.2 X-ray diffraction (XRD) The phase composition of synthesized SnS_2 nanoparticles was characterized by XRD. The XRD characterization shows that both, ethanol- and toluene-treated SnS_2 crystallized in the hexagonal structure. All the diffraction peaks could be indexed according to the standard card (JCPDS No. 23-0677). The prominent peaks at 2Θ = 15.03°, 28.21°, 32.12°, 41.90°, 49.98°, 52.46° correspond to the (001), (100), (101), (102), (110) and (111) planes, respectively. No diffraction peaks belonging to other phases (e.g. SnS, Sn_2S_3) than SnS_2 could be detected, indicating that nanoparticles with single phase hexagonal SnS_2 were obtained; the estimated lattice constants were a = 3.649 Å, c = 5.899 Å. The average crystallite size of the ethanol- and toluene-treated SnS_2 was about 16 nm and 8 nm, respectively, as calculated from the FWHM (001) reflection using the Debye-Scherrer formula [18]:

$$L = \frac{k\lambda}{B \cos\theta} \quad (1)$$

where B is the breadth of the observed diffraction line at its half-intensity maximum, k is the so-called shape factor, which usually takes a value of about 0.9, and λ is the wavelength of X-ray source used in XRD.

By observing Figs. 1 and 2, and taking into account the above results, we can notice that the large faceted nanostructures observed in Fig. 1b actually consist of small SnS_2 hexagonal nanoparticles (see Fig. 2b), while the small spherical nanoclusters in Fig. 1a (prepared with ethanol) are formed also by SnS_2 nanoparticles, but of larger size than those prepared with toluene. Therefore, by varying the type of solvent we can vary both the size of the nanostructures and the nanoparticles obtained.

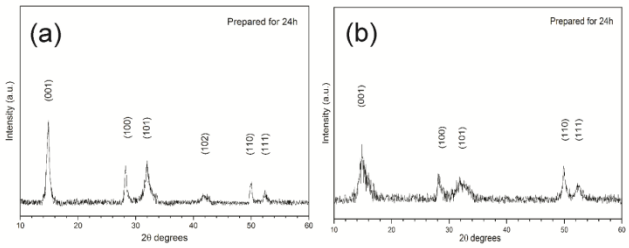

Figure 2 XRD patterns of SnS_2 nanoparticles prepared with (a) ethanol and (b) toluene.

3.3 Micro-Raman spectroscopy The crystal phase of the SnS_2 materials was also determined with micro-Raman spectroscopy. Figure 3 illustrates the Raman spectra of the SnS_2 samples. All of them exhibit a strong Raman peak at around 310-313 cm^{-1}, which corresponds to the A_{1g} mode of the hexagonal phase of SnS_2 [19-21]. Moreover, no Raman peaks attributable to crystalline SnO_2 are visible in Fig. 3, suggesting negligible oxidation of the as-synthesized SnS_2 nanoflakes [22].

However, the first-order E_g mode peaked around 210 cm^{-1} is not observed in the Raman spectra of our materials. This feature has also been reported in the literature and it was attributed to small size of nanoparticles [23-25]. As for the XRD characterization, the difference of the Raman peaks intensity and the FWHM were attributed to the cluster size and the nanoparticle size. That is, toluene produces larger clusters of smaller nanoparticles than ethanol, for which the opposite occurs (smaller clusters of larger nanoparticles).

3.4 Transmission electron microscopy (TEM) Figure 4 shows the TEM images of the SnS_2 nanoparticles synthetized by the hot-injection method. As can be seen from Fig. 4(a) and (b), the solvent plays an important role in the microstructures of the obtained products. A careful observation shows that with the solvent strongly determines the nanostructured morphology. The formation of

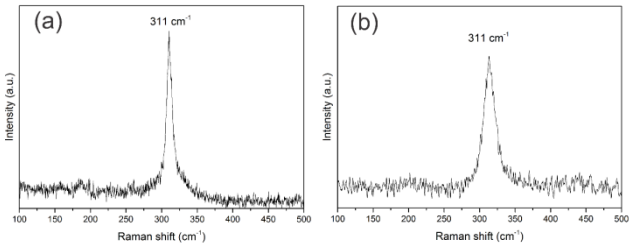

Figure 3 Micro-Raman spectra of SnS_2 nanoparticles prepared with (a) ethanol and (b) toluene.

complex shaped nanostructures usually involves self-assemble or aggregation processes during the solvent evaporation. In our case, the as-prepared SnS_2 nanoparticles form small spherical clusters when ethanol volatilizes away, but in the case of the toluene solvent the as-prepared SnS_2 nanoparticles self-assemble to form rod-shaped two-dimensional structures.

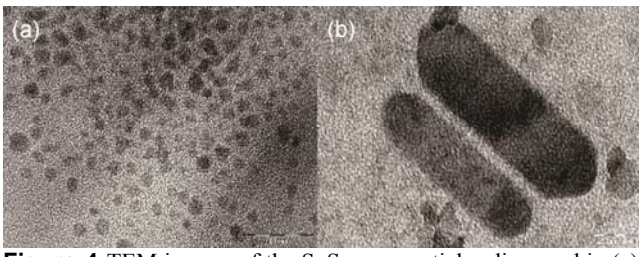

Figure 4 TEM images of the SnS_2 nanoparticles dispersed in (a) ethanol and (b) toluene.

4 Conclusions A low cost hot-injection technique has been successfully applied to obtain single-phase SnS_2 nanoparticles with different morphology and size depending upon the used dispersant (ethanol or toluene) in the rinsing process. The average particle size was 16 and 8 nm, for the ethanol- and toluene- washed particles, respectively. XRD and Raman spectra results indicating that the SnS_2 nanoparticles have a hexagonal crystal structure. We also observed that in the case of toluene evaporation, two- or three-dimensional SnS_2 nanostructures were formed.

Acknowledgements A. Méndez-López thanks to CONACYT-Mexico for providing the Ph.D scholarship. Authors also thank to Mr. Alvaro Guzman for the synthesis of nanoparticles, and also to M. C. Adolfo Tavira (XRD), M. C. Miguel Galvan (Raman Spectroscopy) and M. C. Josué Romero (SEM) for their technical assistance. All the experimental work was carried out at Centro de Investigación y de Estudios Avanzados del IPN (CINVESTAV-IPN).

References

[1] S. Dayal, N. Kopidakis, D. Olson, D. Ginley, and G. Rumbles, Nano. Lett. **10**, 239-242 (2010).
[2] S. Polarz, B. Smarsly, C. Goltner, and M. Antonietti, Adv. Mater. **12**, 1503-1507 (2000).
[3] G. Domingo, R. Itoga, and C. Cannewurf, Phys. Rev. **143**, 536-541 (1966).

[4] J. Morales, V. Perez, J. Santos, and L. Tirado, J. Electrochem. Soc. **143**, 2847-2851 (1996).
[5] L. Sharp, D. Soltz, and B. Parkinson, Cryst. Growth Des. **6**, 1523-1527 (2006).
[6] S. Liu, X. Yin, Q. Hao, M. Zhang, L. Li, L. Chen, Q. Li, Y. Wang, and T. Wang, Mater. Lett. **64**, 2350-2353 (2010).
[7] F. Tan, S. Qu, X. Zeng, C. Zhang, M. Shi, and Z. Wang, Solid State Commun. **50**, 58-61 (2010).
[8] R. Wang and H. Xiao, Mater. Lett. **63**, 1221-1223 (2009).
[9] Y. Lei, S. Song, W. Fan, Y. Xing, and H. Zhang, J. Phys. Chem. C **113**, 1280-1285 (2009).
[10] H. Xiao and Y. Zhang, Mater. Chem. Phys. **112**, 742-744 (2008).
[11] A. Yella, E. Mugnaioli, M. Panthofer, H. Therese, U. Kolb, and W. Tremel. Angew. Chem. Int. Ed. **48**, 6426-6430 (2009).
[12] T. Kim, C. Kim, D. Son, M. Choi, and B. Park, Power Sources **167**, 529-535 (2007).
[13] Y. Lei, S. Song, W. Fan, Y. Xing, and H. Zhang, J. Phys. Chem C **113**, 1280-1285 (2009).
[14] N. Deshpande, A. Sagade, Y. Gudage, C. Lokhande, and R. Sharma, J. Alloys Compd. **436**, 421-426 (2007).
[15] C. Murray, D. Norris, and M. Bawendi, J. Am. Chem. Soc. **115**, 8706-8715 (1993).
[16] S. Kwon and T. Hyeon, Small **7**, 2685-2702 (2011).
[17] A. Sahraneshin, S. Takami, K. Minami, D. Hojo, T. Arita, and T. Adschiri, Prog. Cryst. Growth Charact. Mater. **58**, 43-50 (2012).
[18] C. Gutiérrez, M. Ortega, M. Pérez, M. Espinoza, F. Solís, R. Ortega, L. Silva, V. Castro, and E. Pérez, Beilstein J. Nanotechnol. **5**, 881-886 (2014).
[19] H. Xiao, Y. Zhang, and H. Bai, Mater. Lett. **63**, 809–811 (2009).
[20] Q. Yang, K. Tang, C. Wang, D. Zhang, and Y. Qian, J. Solid State Chem. **164**, 106-109 (2002).
[21] X.L. Gou, J. Chen, and P.W. Shen, Mater. Chem. Phys. **93**, 557-566 (2005).
[22] A.R. Wang and H. Xiao, Mater. Lett. **63**, 1221-1223 (2009).
[23] H. Xiao, Y.C. Zhang, and H. Bai, Mater. Lett. **63**, 809-811 (2009).
[24] Q. Yang, K. Tang, C. Wang, D. Zhang, and Y. Qian, J. Solid State Chem. **164**, 106-109 (2002).
[25] B. Hai, K. Tang, C. Wang, C. An, Q. Yang, G. Shen, and Y. Qian, J. Cryst. Growth **225**, 92-95 (2001).

